Optimization of Waveguide Tapers Capable of Multimode Propagation*

C. C. H. TANG†

Summary—By converting Maxwell's equations, the general case of mode conversion in tapered waveguides is treated by matrix formulation in terms of an infinite set of coupled differential equations with nonuniform coupling coefficients and varying phase constants. An "orthogonalization" or "diagonalization" process is introduced through a nonlinear matrix transformation which is a function of taper length. The general matrix solution of the problem is obtained through a perturbation method in the form of an integral equation of the Volterra type, and the integral equation is solved by an iteration method. In view of the difficulties in finding eigenvalues, the problem is then reduced to the two-mode case, and the mode conversion is obtained in an explicit form revealing certain information which characterizes the choice of "mode-conversion distribution function." Optimization is first obtained through proper choice of the mode-converison distribution function. In an attempt to approximate a Tchebycheff mode-conversion response, further optimization is realized by creating "new zeros" and thereby changing the density of the distribution of zeros in the vicinity of the origin of the mode-conversion curve and the nature of the optimization procedure essentially becomes that of synthesis. Through using the optimized distribution function, a total reduction of about 50 per cent in taper length is realized (when compared with the cosine-squared distribution) for the case of 50-db prescribed-mode discrimination in a taper connecting a $\frac{3}{8}$-in ID waveguide to a 2-in ID waveguide operating in the circular electric mode up to 75 kmc.

I. Introduction

A PERUSAL of recent literature shows that the tapered waveguide capable of multimode propagation has been a subject of interest for the past few years, since in long-distance transmission by use of the low-loss circular electric mode (TE_{01}) in circular waveguide, tapers are necessary in several important applications. Tanaka,[1] expanding the field of conical guide in terms of the eigenfunctions of the uniform circular guide and then matching the fields at the junction, obtained a general expression for a mode conversion through the taper. Solymar,[2] using a similar technique with some approximations, gave the design procedure of a one-section conical taper and a multisection conical taper. Savvirykh,[3] combining perturbation theory with the method of W.K.B., treated the field in the tapered waveguide in terms of an eigenfunction series expansion in an "artificial" orthogonal coordinate system. Unger[4] obtained an improved design of the circular waveguide taper with varying cone angle by using two coupled differential equations. The present paper treats the general case of an infinite set of coupled differential equations in matrix formulation, and the general matrix solution of the problem is obtained through solving an integral equation of the Volterra type by an iteration method. A procedure to create "new zeros" in mode-conversion characteristics is introduced in order to "optimize" the taper for "minimum" length.

The presence of a taper in a waveguide inevitably introduces spurious modes. On the assumption that the taper possesses perfect symmetry and its axis is perfectly straight, only TE_{0n} modes will be excited in the tapered region. If the taper axis has a slight curvature, additional TM_{1n} modes will be excited due to the degeneracy between the TE_{0n} and TM_{1n} modes. Our goal in designing the taper is to reduce the spurious modes to a prescribed level in the operating frequency range with a taper length as short as possible.

To describe electromagnetic fields in a perfectly conducting curved waveguide with nonuniform and arbitrary cross section, we have to solve Maxwell's equations with appropriate boundary conditions. Schelkunoff[5] has shown that certain field problems with complicated boundary conditions can be handled more readily by converting Maxwell's equations into generalized telegraphist's equations. To convert Maxwell's equations into telegraphist's equations, we introduce a complete set of orthogonal functions most appropriate to the particular geometry of the problem in question. Fields within the guide are then expanded in a series in terms of these orthogonal functions of a complete set. Subsituting these fields into Maxwell's equations with due care given to the convergence property of the series on the boundary and taking advantage of the particular orthogonality relations of the functions, we obtain the following generalized telegraphist's equations:

$$\frac{dV_m}{dw} = -\sum_{n=1}^{\infty} Z_{mn} I_n + \sum_{n=1}^{\infty} {}^{V}T_{mn} V_n$$

$$\frac{dI_m}{dw} = -\sum_{n=1}^{\infty} Y_{mn} V_n + \sum_{n=1}^{\infty} {}^{I}T_{mn} I_n,$$

$$m = 1, 2, 3, \cdots, \quad (1)$$

* Received by the PGMTT, April 17, 1961; revised manuscript received, June 23, 1961.

† Bell Telephone Labs., Murray Hill, N. J.

[1] K. Tanaka, "Mode Conversion Through the Tapered Section of Circular Waveguide System," presented at the Congrès Internatl. Circuits et Antennas Hyperfrequences, Paris, France; October, 1957.

[2] L. Solymar, "Monotonic multisection tapers for over-moded circular waveguides," *Proc. IEE*, vol. 106, pt. B, suppl. no. 13, pp. 121, 1959.

[3] S. K. Savvirykh, "On the theory of tapered circular waveguides," *Radioteckh. i Elektron*, vol. 4, pp. 972–1002; April, 1959.

[4] H. Unger, "Circular waveguide taper of improved design," *Bell Sys. Tech. J.*, vol. 37, pp. 899–912; July, 1958.

[5] S. A. Schelkunoff, "Conversion of Maxwell's equations into generalized telegraphist's equations," *Bell Sys. Tech. J.*, vol. 34, pp. 995–1403; September, 1955.

where w is the coordinate along the assumed direction of propagation, Z_{mn} is the self or mutual series impedances, Y_{mn} is the self or mutual shunt admittances, ${}^{V}T_{mn}$ is the "voltage-transfer coefficients," and ${}^{I}T_{mn}$ is the "current-transfer coefficients." V_m and I_m are, respectively, the voltages and currents related to the amplitudes of electric and magnetic intensities associated with each particular function. For the circular-waveguide taper, we choose as the complete set the orthogonal modes of a straight-circular waveguide with perfectly conducting walls and filled with a homogeneous dielectric as in Fig. 1. It is obvious that the

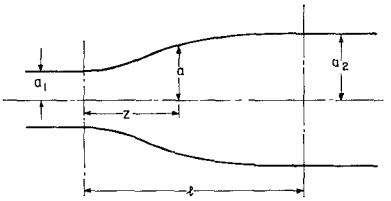

Fig. 1—Circular waveguide taper.

choice is arbitrary, although most appropriate in this case. The infinite set of first-order differential equations (1) with coupling among all possible modes reduces, in this case, to an infinite set with coupling among TE_{0m} modes only and takes the following form[4] in cylindrical cordinates:

$$\frac{dV_m}{dz} = -j\omega\mu I_m + \frac{1}{a}\frac{da}{dz}\sum_{n=1}^{\infty}{}' \frac{2k_mk_n}{k_n^2 - k_m^2} V_n$$

$$\frac{dI_m}{dz} = j\frac{\gamma_m^2}{\omega\mu} V_m + \frac{1}{a}\frac{da}{dz}\sum_{n=1}^{\infty}{}' \frac{2k_mk_n}{k_n^2 - k_m^2} I_n,$$

$$m = 1, 2, 3, \cdots, \quad (2)$$

where the summations are extended over all n except $n=m$. γ_m is the propagation constant of the mth mode, and k_m is the mth root of the Bessel function J_1. If we let A_m and R_m be the amplitudes of the forward and backward waves of a typical mode TE_{0m}, the following equations are always true:

$$V_m = \sqrt{Z_m}\,(A_m + R_m),$$

$$I_m = \frac{1}{\sqrt{Z_m}}(A_m - R_m), \quad (3)$$

where Z_m is the wave impedance of TE_{0m} mode

$$Z_m = \frac{j\omega\mu}{\gamma_m}.$$

Substitution of (3) into (2) results in a new set of equations in A_m and R_m. If the taper is very gradual, we can assume backward waves and multiple reflections negligibly small and obtain the following infinite set of coupled differential equations in forward-wave amplitudes:

$$\frac{dA_m}{dz} = -\gamma_m A_m + \sum_{n=1}^{\infty}{}' \xi_{mn} A_n, \quad (4)$$

where ξ_{mn}'s are the coupling coefficients defined by

$$\xi_{mn} = \frac{1}{a}\frac{da}{dz}\frac{k_mk_n}{k_n^2 - k_m^2}\left(\sqrt{\frac{Z_m}{Z_n}} + \sqrt{\frac{Z_n}{Z_m}}\right). \quad (5)$$

II. General Formulation in Matrix Representation

The infinite set of equations (4) for a section of a tapered waveguide can be conveniently cast in matrix form

$$D\{A\} = [M]\{A\}, \qquad \{A(0)\} = \{C\}, \quad (6)$$

where D, $\{\ \}$ and $[\ ]$ represent, respectively, an operator, a column matrix and a square matrix as follows:

$$D = \frac{d}{dz}, \qquad \{A\} = \begin{bmatrix} A_1(z) \\ A_2(z) \\ A_3(z) \\ \vdots \end{bmatrix},$$

$$[M] = \begin{bmatrix} -\gamma_1(z) & \xi_{12}(z) & \xi_{13}(z) \cdots \\ \xi_{21}(z) & -\gamma_2(z) & \xi_{23}(z) \cdots \\ \xi_{31}(z) & \xi_{32}(z) & -\gamma_3(z) \cdots \\ \vdots & \vdots & \vdots \end{bmatrix}.$$

$[M(z)]$ is assumed to be bounded continuous square-matrix function in a certain interval of the z axis. $\{C\}$ is a column matrix of constants. It is seen that the presence of tapering introduces the coupling terms $\xi_{mn}(z)$ in $[M]$, and the A_m is no longer orthogonal. In a uniform circular waveguide, the coupling coefficients ξ_{mn} vanish, the propagation constants γ_m are independent of z, and the amplitudes A_m form a complete orthogonal set.

For the lossless case, we can show with the aid of the law of conservation of energy that the matrix [M] is, in general, complex and $\xi_{mn} = -\xi_{nm}{}^*$.[6] In our particular case, the elements ξ_{mn} of the matrix are all real, and $\xi_{mn} = -\xi_{nm}$ since the impedances Z_m and Z_n are all real for all modes far away from the cut-off as seen from (5). The propagation constant γ_m is purely imaginary for perfectly conducting tapers and has the form $\gamma = j\beta_m$, where β_m is real. The square matrix $[M]$ then takes the form

$$[M] = \begin{bmatrix} -j\beta_1(z) & C_{12}(z) & C_{13}(z) \cdots \\ -C_{12}(z) & -j\beta_2(z) & C_{23}(z) \cdots \\ -C_{13}(z) & -C_{23}(z) & -j\beta_3(z) \cdots \\ \vdots & \vdots & \vdots \end{bmatrix}, \quad (7)$$

where $\xi_{mn} = C_{mn}$, real functions of z.

[6] The star * implies the complex conjugate.

We now introduce a nonlinear, nonsingular matrix transformation of the following form:

$$\{A\} = [P(z)]\{B(z)\}, \tag{8}$$

in an attempt to obtain a new orthogonal set of amplitudes $B_m(z)$ along the tapered waveguide in at least a localwise sense. Substituting (8) into (6) and following the rules of matrix calculus, we obtain the following:

$$[P]D\{B\} = [M][P]\{B\} - D[P]\{B\}. \tag{9}$$

Multiplication of (9) by $[P]^{-1}$ yields

$$D\{B\} = [Q]\{B\}, \qquad \{B(0)\} = [P(0)]^{-1}\{C\}, \tag{10}$$

where

$$[Q] = [P]^{-1}[M][P] - [P]^{-1}D[P] = [q] - [\epsilon], \tag{11}$$

and

$$[q] = [P]^{-1}[M][P], \qquad [\epsilon] = [P]^{-1}D[P].$$

If the transformation matrix $[P]$ is independent of z, the second term in (11) would vanish and the matrix $[Q]$ is truly diagonal and the B_m's would be orthogonal as seen from (10). In general, the matrix $[Q]$ is not diagonal because of the presence of the term $[P]^{-1}D[P]$, which represents the effect of tapering. However, if $[P]^{-1}D[P]$ can be considered as a small perturbing term to the uniform guide, the matrix differential equation (10) can be solved approximately by perturbation methods. It is worthwhile to note that the transformed-matrix differential equation (10) is of the same form as the original differential equation (6); however, the significance lies in the fact that the weights of the nondiagonal terms of the matrix $[M]$ have been shifted into the diagonal terms of the matrix $[Q]$ by the transformation of (8). Eq. (10), therefore, can yield a more accurate solution by the perturbation method than (6).

To find the matrix $[Q]$, we must first obtain the eigenvectors comprising the diagonalizing matrix $[P]$. This involves the determination of eigenvalues from the secular equation of the matrix

$$|[M] - \lambda[I]| = 0, \tag{12}$$

where $[I]$ is the unit matrix. The values of λ for which the equation is satisfied are the desired eigenvalues. Since $[M]$ is, in general, complex and nonsymmetrical, the eigenvalues and the associated eigenvectors will also, in general, be complex. From (11) and (8) we see that the required transformation matrix $[P(z)]$ also performs the role of a similarity transformation to the matrix $[M(z)]$. If the eigenvalues of the matrix $[M(z)]$ are distinct, there exists a matrix $[P(z)]$ that diagonalizes the matrix $[M(z)]$. The eigenvectors belonging to the corresponding distinct eigenvalues then form an orthonormal basis, *i.e.*,

$$\sum_m P_{mn}P_{ms}^* = \delta_{ns}, \qquad n, s = 1, 2, 3, \cdots, \tag{13}$$

where * denotes the complex conjugate and δ_{ns} the Kronecker delta symbol. When $[P]$ is found, the evaluation of $[P]^{-1}D[P]$ is straightforward. Our task now is to solve the infinite set of coupled differential equations (10) with the appropriate boundary conditions.

The matrix integral of the system of (10) is a square matrix $[B(z)]$, the columns of which are n-linearly-independent solutions of the system. Since each column of the matrix $[B(z)]$ satisfies (10), the matrix integral $[B(z)]$ also satisfies the equation

$$D[B] = [Q][B], \qquad [B(0)] = [I], \tag{14}$$

where $[I]$ is the identity matrix. The formal solution of (10) can now be written in the form

$$\{B\} = [B][P(0)]^{-1}\{C\}. \tag{15}$$

We now seek the solution of system (14)[7] which in view of (11) can be written as

$$D[B] = [q][B] - [\epsilon][B], \qquad [B(0)] = [I]. \tag{16}$$

Under the condition that $[\epsilon]$ may be considered as a very small perturbing matrix relative to the diagonal matrix $[q]$, we can take $[\epsilon][B]$ as the perturbing nonhomogeneous term of the matrix differential equation (16). The approximate solution of (16) in matrix representation is

$$[B] = \exp\left\{\int_0^z [q]dz\right\} - \int_0^z \exp\left\{\int_0^z [q]dz\right\} \cdot \exp\left\{-\int_0^{z'} [q(z')]dz'\right\} [\epsilon(z')][B(z')]dz'. \tag{17}$$

Eq. (17) is a Volterra integral equation of the second kind and can be solved by an iteration method. We obtain, therefore, the final solution of (16) as an infinite series in powers of $[\epsilon]$

$$[B] = \exp\left\{\int_0^z [q]dz\right\}\left\{[I] - \int_0^z \exp\left\{-\int_0^{z'} [q(z')]dz'\right\}[\epsilon(z')]\exp\left\{\int_0^{z'} [q(z')]dz'\right\}dz' + \int_0^z \left[\exp\left\{-\int_0^{z'} [q(z')]dz'\right\}[\epsilon(z')]\exp\left\{\int_0^{z'} [q(z')]dz'\right\}\right] \cdot \left(\int_0^{z'} \exp\left\{-\int_0^{z''} [q(z'')]dz''\right\}[\epsilon(z'')]\exp\left\{\int_0^{z''} [q(z'')]dz''\right\}dz''\right)dz' + \text{terms of higher powers in } [\epsilon]\right\}. \tag{18}$$

[7] See Appendix I.

The uniform convergence of the series in (18) in the closed interval can be shown according to standard methods.[8] The final matrix solution $\{A(z)\}$ is obtained through (18), (15), and (8).

The above general formulation can, in principle, be applied to any number of coupled modes; however, the explicit solutions of the eigenvalues of (12) are already too clumsy to handle even in the case of three coupled modes. Accordingly, only the solution for two coupled modes (TE_{01} and TE_{02}), which have the strongest coupling, will be carried out in the following equation for a gradual taper. Inspection of the coupling coefficient in (5) justifies the preceding statement in addition to the fact that the phase-constant difference is much larger for all other higher-order modes. For TE_{01} and TE_{02} coupling, (12) yields the two eigenvalues

$$\lambda_1 = \tfrac{1}{2}j[-(\beta_1+\beta_2)+\sqrt{(\beta_1-\beta_2)^2+4C_{12}^2}] = -j(\beta-\Gamma) \tag{19}$$

and

$$\lambda_2 = \tfrac{1}{2}j[-(\beta_1+\beta_2)-\sqrt{(\beta_1-\beta_2)^2+4C_{12}^2}] = -j(\beta+\Gamma),$$

where

$$\Gamma = \sqrt{\Delta\beta^2+C_{12}^2} \tag{20}$$

and

$$\Delta\beta = \tfrac{1}{2}(\beta_1-\beta_2); \qquad \beta = \tfrac{1}{2}(\beta_1+\beta_2).$$

$$[B] = \begin{bmatrix} \exp\left\{-j\int_0^z(\beta-\Gamma)dz\right\} & \\ -j\exp\left\{-j\int_0^z(\beta+\Gamma)dz\right\}\int_0^z\frac{d\theta}{dz'} & \\ \cdot\exp\left\{2j\int_0^{z'}\Gamma(z')dz'\right\}dz' & \end{bmatrix}$$

The transformation matrix $[P]$ then takes the form

$$[P] = \begin{bmatrix} j\sqrt{\dfrac{\Gamma+\Delta\beta}{2\Gamma}} & \sqrt{\dfrac{\Gamma-\Delta\beta}{2\Gamma}} \\ \sqrt{\dfrac{\Gamma-\Delta\beta}{2\Gamma}} & j\sqrt{\dfrac{\Gamma+\Delta\beta}{2\Gamma}} \end{bmatrix}. \tag{21}$$

We see that the unitary condition of (13) is satisfied by the $[P]$ matrix, and its determinant is -1 in agreement with the fact that the determinant of an orthonormal matrix can only be $+1$ (corresponding to rotation) or -1 (corresponding to reflection). If use is made of (20) by letting the angle between the sides $\Delta\beta$ and Γ be (2θ), so that $\cos 2\theta = \Delta\beta/\Gamma$, then the matrix $[P]$ of (21) takes the simple form

$$[P] = \begin{bmatrix} j\cos\theta & \sin\theta \\ \sin\theta & j\cos\theta \end{bmatrix}. \tag{22}$$

For small angle (2θ), the variation of (2θ) is directly proportional to that of the coupling coefficient C_{12} and inversely proportional to that of the phase-constant difference $\Delta\beta$ along the taper. Accordingly, this variation of (2θ) can appropriately be interpreted as "mode-conversion distribution" along the taper. The matrix $[\epsilon]$ of (11) in terms of θ becomes a symmetric matrix

$$[\epsilon] = [P]^{-1}D[P] = -j\begin{bmatrix} 0 & \dfrac{d\theta}{dz} \\ \dfrac{d\theta}{dz} & 0 \end{bmatrix}. \tag{23}$$

It is clear now that the coupling to the TE_{01} mode becomes much smaller for higher-order modes. For a gradual taper, we see that $[\epsilon]$ is, indeed, a small perturbing term to the diagonal matrix

$$[q] = [P]^{-1}[M][P] = -j\begin{bmatrix} \beta\mp\Gamma & 0 \\ 0 & \beta+\Gamma \end{bmatrix}. \tag{24}$$

Note that the trace of the diagonalized matrix remains equal to $(\beta_1+\beta_2)$. For a solution to the first order of approximation, we obtain from (18) via (23) and (24)

$$\begin{bmatrix} \exp\left\{-j\int_0^z(\beta-\Gamma)dz\right\} & \\ -j\exp\left\{-j\int_0^z(\beta-\Gamma)dz\right\}\int_0^z\frac{d\theta}{dz'} & \\ \cdot\exp\left\{-2j\int_0^{z'}\Gamma(z')dz'\right\}dz' & \\ \exp\left\{-j\int_0^z(\beta+\Gamma)dz\right\} & \end{bmatrix}. \tag{25}$$

The normalized boundary condition for the two-mode case requires that

$$|\{A(0)\}| = |\{B(0)\}| = |[P(0)]^{-1}\{C\}| = \begin{bmatrix}1\\0\end{bmatrix}, \tag{26}$$

where the vertical bars denote the norm of a vector of complex elements. For a gentle, smooth taper with a mode-conversion distribution function vanishing at both ends of the taper, we obtain the explicit solution for $A_2(l)$ from (8), (22), (15), (25), and (26)

$$A_2(l) = \exp\left\{-j\int_0^l(\beta+\Gamma)dz\right\}\int_0^l\frac{d\theta}{dz}\cdot\exp\left\{2j\int_0^z\Gamma(z')dz'\right\}dz. \tag{27}$$

[8] F. G. Tricomi, "Integral Equations," Interscience Publishers, Inc., New York, N. Y., p. 10; 1957.

Note that $|A_2(l)|$ is essentially in the form of a Fourier transform of $d\theta/dz$. Letting

$$\rho(z) = \int_0^z \Gamma(z')dz' \tag{28}$$

and integrating (27) by parts, we have

$$|A_2(\rho_1)| = \left| \int_0^{\rho_1} (2\theta) e^{2j\rho} d\rho \right|. \tag{29}$$

If we integrate (27) by parts in another way, the following expression is obtained:

$$\begin{aligned} |A_2(\rho_1)| = \Bigg| \frac{1}{2} \Bigg\{ & \left[e^{2j\rho_1} \left(\frac{d\theta}{d\rho} \right)_{\rho=\rho_1} - \left(\frac{d\theta}{d\rho} \right)_{\rho=0} \right] \\ & - \frac{1}{2j} \left[e^{2j\rho_1} \left(\frac{d^2\theta}{d\rho^2} \right)_{\rho=\rho_1} - \left(\frac{d^2\theta}{d\rho^2} \right)_{\rho=0} \right] \\ & + (-1)^{n+1} \left(\frac{1}{2j} \right)^n \left[e^{2j\rho_1} \left(\frac{d^n\theta}{d\rho^n} \right)_{\rho=\rho_1} \right. \\ & \left. - \left(\frac{d^n\theta}{d\rho^n} \right)_{\rho=0} \right] + \cdots \Bigg\} \Bigg|, \end{aligned} \tag{30}$$

where

$$\rho_1 = \rho(l) = \int_0^l \Gamma(z)dz. \tag{31}$$

Eq. (29) is in a form suitable for the computation of "mode discrimination" when the "conversion-distribution function" (2θ) is given in terms of the parameter ρ. Eq. (30), on the other hand, gives us a clue that in order to obtain a higher-mode discrimination, it is advisable to choose a conversion-distribution function with vanishing first and higher derivatives at both taper ends. A detailed discussion will be given in Section V in this respect. When the distribution function (2θ) is chosen, the waveguide radius $a(\rho)$ can be obtained from (5) and (20) and the taper length of the guide $z(\rho)$ from (28).

III. The Choice of Conversion Distribution Function

It is evident that the choice of distribution function is not unique. Under the stipulation that the function itself vanishes at both ends as expressed in (8), (22) and (26), a simple choice of such a function in the form of an infinite series in (ρ/ρ_1) is

$$2\theta = K_n \sin^n \left(\frac{\pi\rho}{\rho_1} \right), \tag{32}$$

where $\sin(\pi\rho/\rho_1)$ can be considered as a "generating" function, and n may or may not be an integer. Substituting (32) into (29) and using (47) in Appendix II, we can show that the mode discrimination is given by

$$|A_2(\rho_1)| = \left| C(2\cdot 4\cdot 6\cdot \cdots \cdot n)^2 \frac{ab^n(e^{a\rho_1} - 1)}{\rho_1 \prod_{s=0}^{n} (a^2 + s^2b^2)} \right|, \quad n \text{ even} \tag{33a}$$

$$|A_2(\rho_1)| = \left| C(1\cdot 3\cdot 5\cdot \cdots \cdot n)^2 \frac{b^{n+1}(e^{a\rho_1} + 1)}{2 \prod_{s=1}^{n} (a^2 + s^2b^2)} \right|, \quad n \text{ odd}, \tag{33b}$$

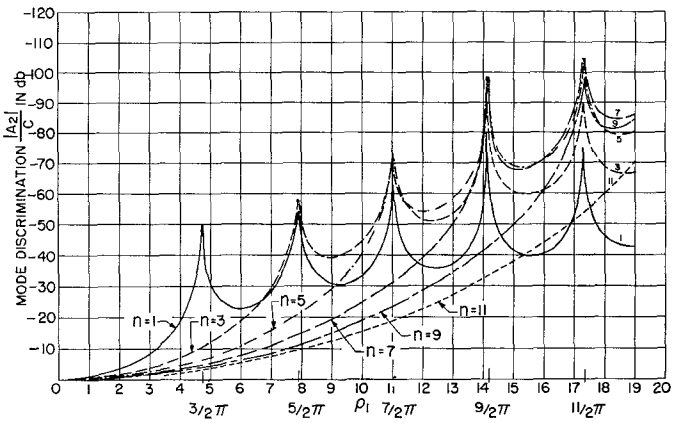

(a)

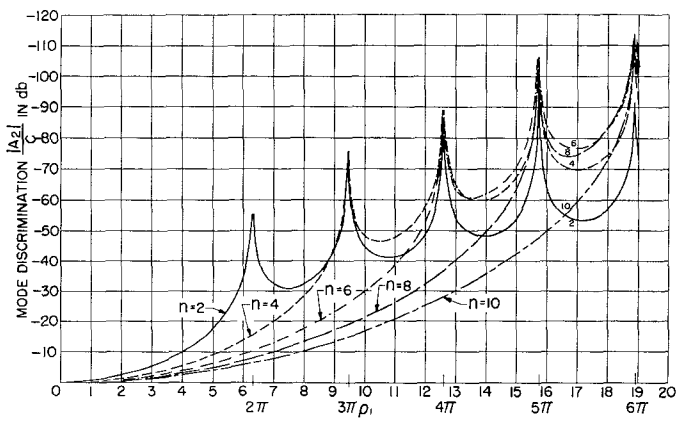

(b)

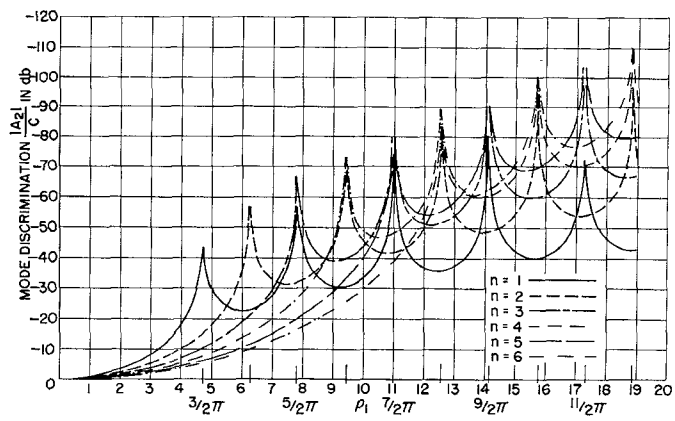

(c)

Fig. 2—(a)–(c) Mode conversion in waveguide tapers.

where

$$a = 2j, \qquad b = \frac{\pi}{\rho_1}, \quad \text{and} \quad C = \frac{2k_m k_n}{k_n^2 - k_m^2} \log \frac{a_2}{a_1}. \tag{34}$$

and k_m and k_n are defined in (2). It is evident from (33) that C corresponds to the mode conversion of a step discontinuity in the diameter of the waveguide. For cases where n is noninteger, general solutions for the mode discrimination in closed form are impossible, and we have to resort to numerical integration. Eq. (33) for integral values of n are plotted in Fig. 2(a)–2(c).

It is seen from these figures that there is always an "optimum" integer n which minimizes the length of a taper for a prescribed discrimination. Alternatively, if we prescribe the taper length, there is always an optimum integer n that provides the highest-mode discrimination. From Fig. 2(a) we see that, for a fixed taper length of $\rho_1 = 18.5$, optimum discrimination occurs for $n = 7$. On the other hand, if we prescribe a -50-db mode discrimination within a frequency range up to 75 kMc, the required minimum length of the taper for the case ($a(0) = 7''/16$ and $a(l) = 1''$) is about 3 ft[4] using $n = 2$, but only about 2 ft using $n = 3$ as shown in Fig. 3. The actual computation of radius a and length z is shown in Appendix II.

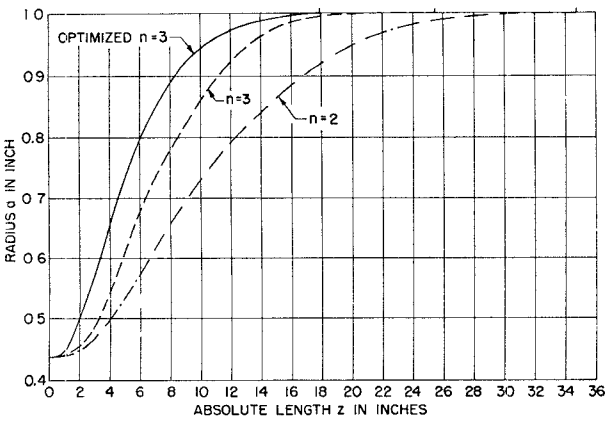

Fig. 3—Comparison of profile of tapers of same mode conversion (50 db).

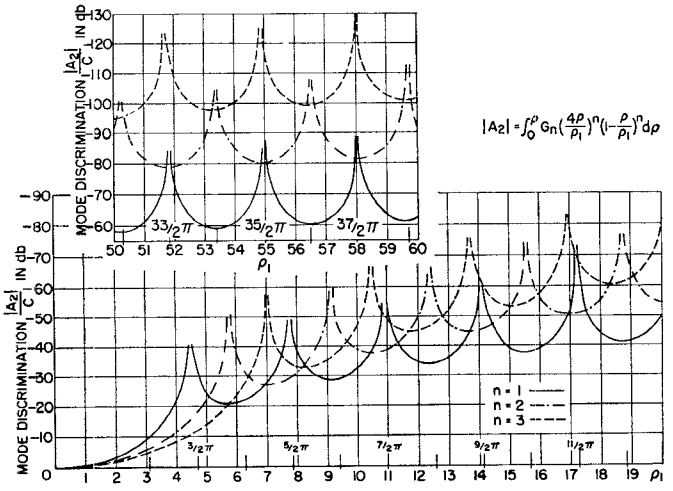

Fig. 4—Mode conversion in waveguide tapers.

Another simple choice for the distribution function is a polynomial in (ρ/ρ_1)

$$2\theta = G_n \left(\frac{4\rho}{\rho_1}\right)^n \left(1 - \frac{\rho}{\rho_1}\right)^n, \tag{35}$$

where the "generating" function is $(4\rho/\rho_1)(1-\rho/\rho_1)$, and n may or may not be an integer. Evaluating the integral of (29) for (35) with integer n, it can be shown that the mode discrimination is equal to

$$\begin{aligned}
|A_2(\rho_1)| &= \left| \frac{3 \cdot C}{2 \cdot \rho_1} \left(\frac{2}{\rho_1}\right)^2 \left[\left(\frac{\rho_1}{a^2} (e^{a\rho_1} + 1) \right. \right. \right. \\
&\qquad \left. \left. \left. - \frac{2}{a^3} (e^{a\rho_1} - 1) \right] \right| \qquad \text{for } n = 1, \\
|A_2(\rho_1)| &= \left| \frac{3 \cdot 5 \cdot C}{2^3 \cdot \rho_1} \left(\frac{2}{\rho_1}\right)^4 \left[\left(\frac{2\rho_1^2}{a^3} + \frac{24}{a^5} \right) (e^{a\rho_1} - 1) \right. \right. \\
&\qquad \left. \left. - \frac{12\rho_1}{a^4} \cdot (e^{a\rho_1} + 1) \right] \right| \qquad \text{for } n = 2, \\
|A_2(\rho_1)| &= \left| \frac{5 \cdot 7 \cdot C}{2^4 \cdot \rho_1} \left(\frac{2}{\rho_1}\right)^6 \left[\frac{6\rho_1}{a^4} \left(\rho_1^2 + \frac{60}{a^2} \right) (e^{a\rho_1} + 1) \right. \right. \\
&\qquad \left. \left. - \frac{72}{a^5} \cdot \left(\rho_1^2 + \frac{10}{a^2} \right) (e^{a\rho_1} - 1) \right] \right| \qquad \text{for } n = 3,
\end{aligned} \tag{36}$$

where C is defined in (34). Eq. (36) is plotted in Fig. 4. It can be shown that both (33) and (36) have the value unity times C at $\rho_1 = 0$, as they should. Eqs. (33) have all their zeros at multiples of $\pi/2$; on the other hand, (36) has its initial zeros shifted closer toward the origin $\rho_1 = 0$, as shown in Fig. 4. Inspection of Fig. 4 shows that the zeros at large values of ρ_1 also gradually shift to positions at multiples of $\pi/2$ as (33) do. Comparison of Fig. 2 and Fig. 4 for curves of corresponding values of n shows that the sine distribution has better over-all discrimination than the polynomial distribution, except in the region between $\rho_1 = 0$ and the first zero of (33).

IV. Optimization

In an attempt to further generalize and optimize the mode-conversion distribution function, we expand it in a symmetrical Fourier series (with the origin of the coordinate system shifted to the center of the taper)

$$2\theta = \sum_{m=0}^{\infty} D_m \cos m \left(\frac{\pi\rho}{\rho_1}\right). \tag{37}$$

With suitably-chosen coefficients D_m's, it is obvious that

(37) can include all cases described by (32) and (35). Substituting (37) into (29), we have

$$|A_2(\rho_1)| = \left| \int_{-\rho_1/2}^{\rho_1/2} \sum_{m=0}^{\infty} D_m \cos m\left(\frac{\pi\rho}{\rho_1}\right) e^{2j\rho} d\rho \right|$$

$$|A_2(\rho_1)| = \left| \sum_{m=0}^{\infty} \frac{2D_m \cos m\frac{\pi}{2}(e^{a\rho_1}-1)}{a^2+m^2b^2} \right|, \quad m \text{ even} \quad (38a)$$

$$|A_2(\rho_1)| = \left| \sum_{m=1}^{\infty} \frac{mbD_m \sin m\frac{\pi}{2}(e^{a\rho_1}+1)}{a^2+m^2b^2} \right|, \quad m \text{ odd} \quad (38b)$$

where a and b are defined in (34). It is important to note that only odd or even values of m are required to represent the mode-conversion distribution function given in (33), depending on whether n is odd or even. Equating (38) to (33) for the corresponding case, we can obtain the D_m in (38) as shown in Table I. It is interesting to note that the ratio of D_m's for a particular n correspond to the coefficients of the binomial expansion. We are now in a position to further optimize the mode-conversion curve defined by (33), using the values of Table I as a guide. The aim is to reshape the mode-conversion curve in such a way that the first few maxima of the "side lobes" of (33) will be leveled and at the same time lowered optimally. Before carrying out the optimizing procedure, it is appropriate at this point to discuss the incentive for this further optimization in more detail in the following paragraph.

TABLE I

$n=0$	$D_0 = \frac{C}{\rho_1}$.		
$n=2$	$D_0 = \frac{C}{\rho_1}$,	$D_2 = \frac{C}{\rho_1}$.	
$n=4$	$D_0 = \frac{C}{\rho_1}$,	$D_2 = \frac{4}{3}\cdot\frac{C}{\rho_1}$,	$D_4 = \frac{1}{4}\cdot\frac{C}{\rho_1}$.
$n=1$	$D_1 = \frac{\pi C}{2\rho_1}$.		
$n=3$	$D_1 = \frac{9}{8}\cdot\frac{\pi C}{2\rho_1}$,	$D_3 = \frac{1}{3}\cdot\frac{9}{8}\cdot\frac{\pi C}{2\rho_1}$.	
$n=5$	$D_1 = \frac{75}{64}\cdot\frac{\pi C}{2\rho_1}$,	$D_3 = \frac{1}{2}\cdot\frac{75}{64}\cdot\frac{\pi C}{2\rho_1}$,	$D_5 = \frac{1}{10}\cdot\frac{75}{64}\cdot\frac{\pi C}{2\rho_1}$.

The class of distribution functions that we have been considering have the property that the distribution function and all its derivatives are single-valued, uniformly bounded, and continuous in the interval of interest. Any distribution function of this class can be transformed to a general form in terms of the zeros of the function. With the coordinate origin at the center of the taper, the function of interest has the form

$$2\theta = f(\rho)\left[\rho^2 - \left(\frac{\rho_1}{2}\right)^2\right]^n, \quad (39)$$

where $f(\rho)$ is an even function due to the symmetry of the function (2θ), and $f(\rho)$ does not vanish at the taper ends $(\rho = \pm\rho_1/2)$ or any other value of ρ in the interval. Taylor[9] has shown that the Fourier transform of (39) has the following asymptotic form as ρ_1 approaches infinity:

$$F(\rho_1) \sim f\left(\frac{\rho_1}{2}\right)\Gamma(n+1)\frac{\cos\left(\rho_1 - \frac{n+1}{2}\pi\right)}{(\rho_1)^{n+1}}. \quad (40)$$

It is, therefore, seen that the mode discrimination of very long tapers is only trivially different, no matter what form the distribution function has. On the other hand, as we have seen earlier, the initial slope of the function and accordingly the value of n are of considerable importance in "optimizing" the taper. The initial slope of the function (2θ) determines the positions of the zeros near the origin of the mode discrimination curve $A_2(\rho)$. The smaller the initial slope, the further will the first zero be from the origin. Likewise, the value of n alters the zero positions, since n changes the slope of the function. Eq. (40) indicates clearly that spurious mode conversion or discrimination decays as $1/|\rho_1|^{n+1}$ and zeros appear at $\rho_1 = n(\pi/2)$ at large values of ρ_1. Inspection of (33), (36) and (38) confirms this decay rate and the position of zeros at large values of ρ_1. At this point, it is particularly appropriate to compare this decay rate with the nondecaying characteristics of the Tchebycheff polynomial of infinite degree. If we are to simulate the Tchebycheff polynomial of infinite degree by the function of (40), we see that the only choice to make (40) nondecaying is to make $n = -1$. However, for this choice of n, the function of (39) will have poles at the taper ends and will no longer be uniformly bounded. This violates our basic requirement, and, therefore, it is clear that a smooth transition taper with its mode-conversion characteristics described by a Tchebycheff polynomial of infinite degree is unrealizable. In fact, this unrealizability is simply a consequence of the law of conservation of energy. This is why even

[9] T. T. Taylor, "Design of line-source antenna for narrow bandwidth and low side lobes," IRE TRANS. ON ANTENNAS AND PROPAGATION, vol. AP-3, pp. 16–28; January, 1955.

in the transmission line case either steps[10] have to be introduced at taper ends or a modified[11] Tchebycheff polynomial of infinite degree has to be used in the synthesis procedure. Although the frequency range of the design using infinite degree Tchebycheff polynomial extends to infinity, for band-pass applications this is unnecessary. Accordingly, the Tchebycheff design is optimum only in the sense of infinite bandwidth, even for a transmission-line taper.

From the above exposition, we see that in order to further optimize, we need to "flatten" or "level" the decay rate of the first few "minor lobes" of the mode-conversion curve as much as permissible, after choosing the "optimum" value of n for a prescribed discrimination level from Fig. 2(c). It is clear that the nature of this procedure essentially becomes that of synthesis. At first sight, this might look rather aimless if we do it in a heuristic way by adjusting the coefficients D_m of (38). Knowing, however, that the shape of the mode-conversion curve of (38) depends very much on the density of the distribution of zeros near the origin, we are thus led to create an extra "zero" at such a position that the "side lobes" near the origin will be leveled and at the same time optimally lowered. It is important to note that the new zeros will be introduced by properly choosing the coefficients D_m in (38), while the original zeros were determined only by the term $(e^{a\rho_1} \pm 1)$. This will be done first for $n=3$. With reference to (38b), we have

$$D_1'\left[3^2 - \left(\rho_1 \frac{2}{\pi}\right)^2\right] - 3D_3'\left[1^2 - \left(\rho_1 \frac{2}{\pi}\right)^2\right] = 0, \tag{41}$$

where

$$D_m = \frac{bc}{2} D_m' = \frac{\pi C}{2\rho_1} D_m'.$$

With (41) and the boundary condition that $A_2(0) = C$,

$$\left(D_1' - \frac{D_3'}{3}\right) = 1. \tag{42}$$

We can solve for the required coefficients D_1' and D_3' when the position of the new zero is intelligently selected. Inspection of Fig. 2(a) for $n=3$ shows that it is advisable to locate the "new zero" around $\rho_1 = 6(\pi/2)$ in order to achieve the desired results. With this value of ρ_1, we get $D_1' = 1.09375$ and $D_3' = 0.28125$ from (41) and (42). A plot of (38) with these values of D_1' and D_3' as shown in Fig. 5 indeed gives the desired results. Fig. 6, showing the relation between the position of the new zero and the maximum of the maxima of the side lobes, also confirms the fact that the optimum location of the new zero should be in the vicinity of $6(\pi/2)$. Mode-conversion curves for

$$\cos^3\left(\frac{\pi\rho}{\rho_1}\right) \quad \text{and} \quad \left[\frac{\rho}{\rho_1}\left(1 - \frac{\rho}{\rho_1}\right)\right]^3$$

are also plotted in Fig. 5 for comparison. It is seen that the optimized conversion curve does have its first few side lobes maxima leveled, and the maxima of the remaining side lobes decay according to a rate asymptotically proportional to $1/\rho_1^4$. The improvement is about another 30 per cent reduction in taper length for 50-db discrimination. The actual optimized length of the taper is plotted in Fig. 3 for comparison. Through using the optimized $\cos^3(\pi\rho/\rho_1)$ distribution function, a total reduction of about 50 per cent in taper length is realized for the case of 50-db prescribed mode discrimination in a taper connecting a $\frac{7}{8}$-in ID waveguide to a 2-in ID waveguide.

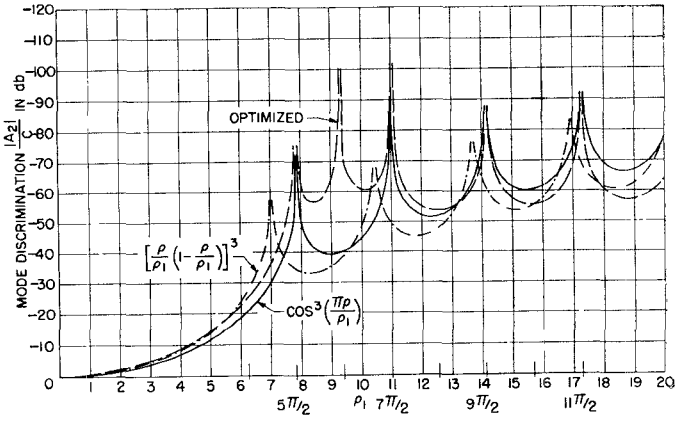

Fig. 5—Comparison of mode conversion in waveguide tapers.

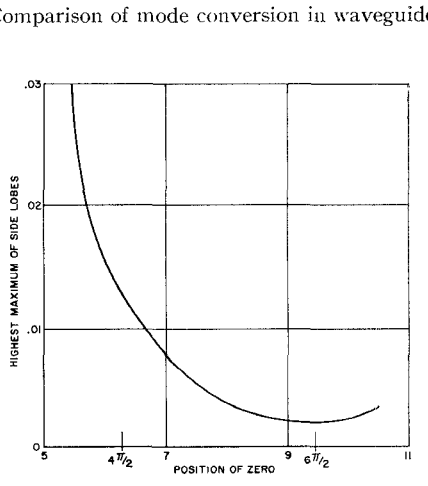

Fig. 6—Optimization of the position of new zero.

[10] R. W. Klopfenstein, "A transmission line taper of improved design," PROC. IRE, vol. 44, pp. 31–35; January, 1956

[11] R. E. Collin, "The optimum tapered transmission line matching section," PROC. IRE, vol. 44, pp. 539–548; April, 1956.

The same procedure can be applied, for example, to the $n=5$ case and we have

$$D_1'\left[3^2-\left(\rho_1\frac{2}{\pi}\right)^2\right]\left[5^2-\left(\rho_1\frac{2}{\pi}\right)^2\right]$$
$$-3D_3'\left[1^2-\left(\rho_1\frac{2}{\pi}\right)^2\right]+\left[5^2-\left(\rho_1\frac{2}{\pi}\right)^2\right]$$
$$+5D_5'\left[1^2-\left(\rho_1\frac{2}{\pi}\right)^2\right]\cdot\left[3^2-\left(\rho_1\frac{2}{\pi}\right)^2\right]=0 \qquad (43)$$

and

$$\left[D_1'-\frac{D_3'}{3}+\frac{D_5'}{5}\right]=1, \qquad (44)$$

where

$$D_m=\frac{\pi C}{2\rho_1}D_m'.$$

Inspection of Fig. 2(a) shows that the logical choice for the location of the new zero is at $\rho_1=8(\pi/2)$. In this case, however, we have only two equations for three unknowns. It is necessary to assume an appropriate value of D_1' so that D_3' and D_5' can be determined. The first suitable choice of D_1' might be $D_1'=75/64$ obtained from Table I for the $n=5$ case. Calculation shows again that the new zero should indeed be around $\rho_1=8(\pi/2)$, and the optimum choice of D_1 is indeed (75/64). This case is shown in Fig. 7 together with the $\cos^5(\pi\rho/\rho_1)$ case for comparison.

Further investigation of the $n=5$ case reveals a better value for D_1' because we can now create two new zeros in view of the extra undetermined coefficient. The assignment of the second zero will give us an extra equation and thus determine the three coefficients uniquely. A judicial choice of two zeros at $\rho_1=8(\pi/2)$ and $\rho_1=10(\pi/2)$, respectively, should yield even better mode discrimination at a fixed taper length than the above case. This result is also plotted in Fig. 7 for comparison and shows that the prediction is valid. A relocation of the first "created zero" at $\rho_1=7.72(\pi/2)$ gives the best discrimination for this case, as shown in Fig. 7. Accordingly, it is seen that we can further optimize a taper by creating new zeros near the first few zeros of the mode-conversion curve, and the number of new zeros allowed to be created increases directly as the number of undetermined coefficients. On the other hand, the freedom to have more created zeros is only available for higher values of n which dictates higher mode discrimination and longer taper lengths.

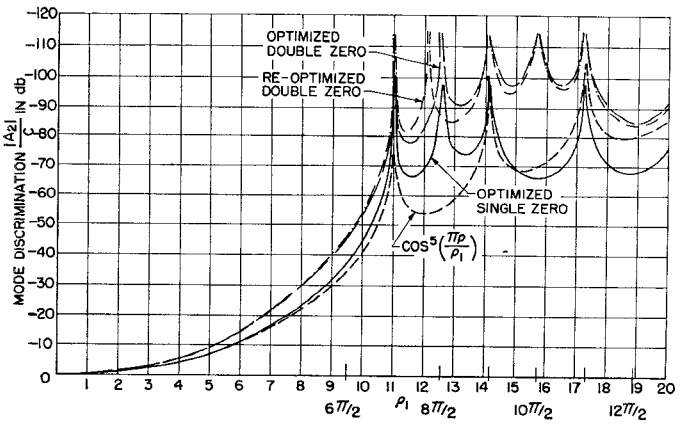

Fig. 7—Comparison of mode conversion in waveguide tapers.

V. Conclusions

In an attempt to approximate a Tchebycheff mode-conversion response in a wideband waveguide taper, we optimize the taper by creating new zeros in the mode-conversion response. This response had been initially selected to yield the "shortest" taper length in the "sine or cosine distribution function family" at a prescribed level of mode discrimination.

We note that the first and second derivative of a distribution function with ratio $D_3/D_1=\frac{1}{3}$ [this is the $\cos^3(\pi\rho/\rho_1)$ case] vanish at the taper ends, but those with ratios other than $\frac{1}{3}$ do not vanish. Thus, change of end slopes evidently is a consequence of the addition of new zeros in the mode-conversion curve, since the end slopes are closely related to the position and density of the zero distribution near the origin. Because the optimized distribution functions do not have vanishing derivatives at the taper ends, it is seen that the distribution functions with vanishing derivatives at the taper ends may not be most desirable. We now return to (30) for further information in this respect. It can be easily shown that for the symmetrical distribution functions we used, the nth derivatives at the taper ends decreases as $1/\rho_1^{n+1}$, where ρ_1 is the equivalent taper length. This implies that longer tapers have smaller derivatives and that the $(n+1)$th derivative is smaller than the nth derivative. Investigation of (30) also shows that if a symmetrical distribution function has its first and second derivative vanishing, the third derivative will represent a significant part of the mode conversion. On the other hand, if the first two derivatives are nonvanishing but very small, the total mode conversion may still be smaller than the vanishing derivative case due to alternate + signs and − signs in the real and imaginary parts of (30).

From what has been shown here, it is obvious that we cannot claim to have synthesized the absolute optimum taper, but we can claim the taper to be very close to the absolute optimum. The procedure discussed above

may lead to a further optimization, but it is quite clear that the small reduction of taper length due to such a procedure might not justify the amount of computational labor involved. The starting point is still (32). For instance, for a certain prescribed spurious mode level, there is in (32) an "optimum" n which may be noninteger. The evaluation of (29) with a distribution function of noninteger power will require numerical integration, and the evaluation of the radius and length of the taper as shown in Appendix II will again require numerical integration.

Appendix I

If the matrix $[\delta]$ can be considered as a perturbing matrix to a matrix $[N]$, the matrix exponential $e^{[N]+[\delta]}$ can be expressed in several ways. If $[N]$ and $[\delta]$ commute, then

$$e^{[N]+[\delta]} = e^{[N]}e^{[\delta]}.$$

Considering the general case where $[N]$ and $[\delta]$ do not commute, we can write

$$e^{[N]+[\delta]} = [I] + \sum_{k=1}^{\infty} \frac{([N] + [\delta])^k}{k!}.$$

By expanding the series, we can collect the terms in powers of the perturbing term $[\delta]$ in the form of

$$e^{[N]+[\delta]} = e^{[N]} + \sum_{k=1}^{\infty} [\delta]^k f_k([N]).$$

This, however, cannot be accomplished in a neat fashion, and it is necessary to solve equations of the form of (16) by perturbation techniques.

Appendix II

The coefficient C_{12} is obtained from (5) under the stipulation of the TE_{01} and TE_{02} modes that are far away from cut-off, and it takes the following simple form:

$$C_{12} = \frac{1}{a}\frac{da}{dz}\cdot\frac{2k_1k_2}{k_2^2 - k_1^2} = \frac{k}{a}\frac{da}{dz},$$

where

$$k = \frac{2k_1k_2}{k_2^2 - k_1^2}.$$

From the preceding equation and (20) and (28), we have

$$\int_{a_1}^{a} \frac{da}{a} = \int_0^{\rho} \frac{2\theta}{k}\, d\rho \tag{45}$$

for a gentle taper.

For $2\theta = K_n \sin^n(\pi\rho/\rho_1)$, (45) becomes

$$\log\frac{a}{a_1} = \frac{K_n}{k}\left[-\frac{\sin^{n-1}\left(\frac{\pi\rho}{\rho_1}\right)\cos\left(\frac{\pi\rho}{\rho_1}\right)}{n\left(\frac{\pi}{\rho_1}\right)} + \frac{n-1}{n}\int_0^{\rho}\sin^{n-2}\left(\frac{\pi\rho}{\rho_1}\right)d\rho\right]. \tag{46}$$

Boundary conditions require that

$$K_n = \frac{1}{2}\left[1\cdot\frac{3}{2}\cdot\frac{5}{4}\cdots\frac{n}{n-1}\frac{\pi k\log\frac{a_2}{a_1}}{\rho_1}\right], \quad n \text{ odd}$$

$$K_n = \frac{2}{1}\cdot\frac{4}{3}\cdot\frac{6}{5}\cdots\frac{n}{n-1}\frac{k\log\frac{a_2}{a_1}}{\rho_1}, \quad n \text{ even}. \tag{47}$$

Substitution of (47) into (46) yields for

$$\frac{1}{2}\left[1 - \cos\left(\frac{\pi\rho}{\rho_1}\right)\right]\log\frac{a_2}{a_1}$$

$n = 1$: $a = a_1 e$

$$\left[\frac{\rho}{\rho_1} - \frac{1}{2\pi}\sin 2\pi\frac{\rho}{\rho_1}\right]\log\frac{a_2}{a_1}$$

$n = 2$: $a = a_1 e$

$$\frac{1}{2}\left[1 - \frac{3}{2}\cos\left(\frac{\pi\rho}{\rho_1}\right) + \frac{1}{2}\cos^3\left(\frac{\pi\rho}{\rho_1}\right)\right]\log\frac{a_2}{a_1}$$

$n = 3$: $a = a_1 e$. (48)

The actual length of the taper in terms of the parameters ρ_1 is obtained from (28). For a gentle taper it is

$$z = \frac{1}{k_2^2 - k_1^2}\left[4\beta_0\int_0^{\rho} a^2 d\rho - \frac{\rho}{\beta_0}(k_2^2 + k_1^2) - \frac{1}{4\beta_0^3}(k_2^4 + k_1^4)\int_0^{\rho}\frac{d\rho}{a^2}\right], \tag{49}$$

where β_0 is the phase constant in free space. The last term in (49) is negligibly small, in general. Substitution of (48) into (49) gives

$$n = 1: \quad z = \frac{4\beta_0 a_1/a_2\rho_1}{\pi(k_2^2 - k_1^2)}\left[\left(1 + \frac{\alpha^2}{4} + \frac{\alpha^4}{64}\right)x - \left(\alpha + \frac{\alpha^5}{150}\right)\sin x + \left(\frac{\alpha^2}{8} + \frac{\alpha^4}{128}\right)\sin 2x + \left(\frac{\alpha^3}{18} + \frac{\alpha^5}{450}\right)\sin^3 x + \frac{\alpha^4\cos^3 x\sin x}{96} - \frac{\alpha^5\cos^4 x\sin x}{600}\right] - \frac{\rho(k_2^2 - k_1^2)}{\beta_0}.$$

where

$$x = \frac{\pi\rho}{\rho_1} \quad \text{and} \quad \alpha = \log_e \frac{\alpha_2}{\alpha_1}$$

$n = 2$:

$$z = \frac{2a_1^2\beta_0\rho_1}{\pi(k_2^2 - k_1^2)} \left\{ e^{qy} \left[\frac{1}{q} - \left(\frac{8q + q^3}{8q^2 + 8} \right) (q \sin y - \cos y) \right. \right.$$

$$+ \frac{12q + q^3}{48} - \left(\frac{12q^2 + q^4}{q^2 + 4} \right) (q \cos 2y + 2 \sin 2y)$$

$$\left. - \frac{q^4(2 \sin 2y + q \cos 2y + 4 \sin 4y + q \cos 4y)}{192(q^2 + 16)} \right]$$

$$- \left[\frac{1}{q} + \frac{8q + q^3}{8(q^2 + 1)} + \frac{12q + q^3}{48} - \frac{12q^3 + q^5}{q^2 + 4} \right.$$

$$\left. \left. - \frac{q^5}{96} \right] \right\} - \frac{\rho(k_2^2 - k_1^2)}{\beta_0},$$

where

$$y = 2\pi \frac{\rho}{\rho_1} \quad \text{and} \quad q = \frac{1}{\pi} \log_e \frac{a_2}{a_1}.$$

$n = 3$:

$$z = \frac{4\beta_0 a_1 a_2 \rho_1}{\pi(k_2^2 - k_1^2)} \left[x - \frac{3}{2} \alpha \sin x + \frac{9}{16} \alpha^2 \left(\frac{x}{3} + \frac{\sin 2x}{2} \right) \right.$$

$$+ \left(\frac{1}{2} \alpha - \frac{27}{112} \alpha^3 + \frac{81}{1120} \alpha^5 \right) \left(\sin x - \frac{\sin^3 x}{3} \right)$$

$$- \left(\frac{31}{48} \alpha^2 - \frac{99}{256} \alpha^4 - \frac{81}{6144} \alpha^6 \right) \left(\frac{3x}{8} + \frac{3 \sin 2x}{16} \right.$$

$$\left. + \frac{\cos^3 x \sin x}{4} \right) + \left(\frac{\alpha^2}{8} - \frac{81}{512} \alpha^4 + \frac{81}{5120} \alpha^6 \right)$$

$$\cdot \frac{\cos^5 x \sin x}{6} + \frac{9\alpha^4}{64} \frac{\sin x \cos^7 x}{8} + \left(\frac{45}{112} \alpha^3 - \frac{243}{8960} \alpha^5 \right)$$

$$\left. \cdot \frac{\cos^4 x \sin x}{5} + \left(\frac{27}{256} \alpha^5 - \frac{3}{16} \alpha^3 \right) \frac{\sin x \cos 6x}{7} \right] - \frac{\rho(k_2^2 - k_1^2)}{\beta_0},$$

ACKNOWLEDGMENT

The author is indebted to Miss E. G. Cheatham for her assistance in carrying out most of the computations and to Mrs. M. O. Czarnomski for carrying out the initial phase of computation.

Correspondence

A Broad-Band Coaxial Ferrite Switch*

A broad-band strip-line reflective ferrite switch has been described by Johnson and Wiltse,[1] who also referred to the possibility of a similar switch in coaxial line. This note describes a coaxial on-off switch which will operate over the band 2500–4100 Mc; two such units can be combined to make a two-way switch. An isolation of 40 db was achieved, with a very low loss for the transmitting path, which, in both these devices, was obtained by magnetizing the ferrite well beyond the value for isolation.[2]

Each switching element employed a small slug of a developmental ferrite (B_{sat}=2280 gauss) which completely filled a half-inch section of air spaced coaxial line of 9/32 inch outer diameter and $\frac{1}{8}$ inch inner diameter, the ends of which were directly coupled to Type "C" coaxial connectors. Fig. 1 shows the attenuation obtained with a field of about 400 oe compared with pads of approximately 30 db and 40 db, while Fig. 2 shows the attenuation obtained with a field of about 2500 oe compared with a 3-db pad. The attenuation of about 40 db was obtained at 100°C in a convection cooled solenoid, but greater attenuation was achieved at lower temperatures. The VSWR under reflecting conditions in Fig. 3 is about 0.15, but a lower value may be obtained over a smaller bandwidth. The solenoid power required was rather high, but was reduced by constructing the coaxial line of iron with a brass section in the position of the ferrite slug. Permanent magnet bias can also be used without unduly slowing the switching speed.

Fig. 4 shows the variation in the position of the effective short-circuit planes in front of a slug of a similar ferrite material. A two-way switch may be constructed therefore by arranging for a high impedance to appear at the T junction. Two ferrite slugs were used in the top of the "T," one of which was magnetized for isolation and the other for transmission at any instant. The transmission loss for the two-way switch is shown in Fig. 5.

The development of this switch was part of the work done under a contract for the Admiralty.

* Received by the PGMTT, June 5, 1961.

[1] C. M. Johnson and J. C. Wiltse, "A broad-band ferrite reflective switch," IRE TRANS. ON MICROWAVE THEORY AND TECHNIQUES, vol. MTT-8, pp. 466–467; July, 1960.

[2] The General Electric Company, Ltd., Brit. Patent Application No. 19948/59; June 10, 1959.